

Effect of Molecular Weight on the Mechanical and Electrical Properties of Block Copolymer Electrolytes

Mohit Singh,[†] Omolola Odusanya,^{†,‡} Gregg M. Wilmes,^{‡,§} Hany B. Eitouni,^{‡,§} Enrique D. Gomez,[‡] Amish J. Patel,[‡] Vincent L. Chen,[‡] Moon Jeong Park,[†] Panagiota Fragouli,[‡] Hermis Iatrou,[‡] Nikos Hadjichristidis,[‡] David Cookson,[#] and Nitash P. Balsara^{*,†,‡,§}

Environmental Energy Technologies Division, Lawrence Berkeley National Laboratory, University of California, Berkeley, Berkeley, California 94720; Department of Chemical Engineering, University of California, Berkeley, Berkeley, California 94720; Materials Sciences Division, Lawrence Berkeley National Laboratory, University of California, Berkeley, Berkeley, California 94720; Department of Chemistry, University of Athens, Panepistimiopolis Zografou, 157 71 Athens, Greece; and Australian Synchrotron Research Program, Bldg 343, Advanced Photon Source, Argonne National Laboratory, 9700 South Cass Avenue, Argonne, Illinois 60439

Received December 25, 2006; Revised Manuscript Received March 23, 2007

ABSTRACT: The relationship between ionic conductivity, morphology, and rheological properties of polystyrene-*block*-poly(ethylene oxide) copolymers (SEO) doped with a lithium salt, Li[N(SO₂CF₃)₂], is elucidated. We focus on lamellar samples with poly(ethylene oxide) (PEO) volume fractions, ϕ , ranging from 0.38 to 0.55, and PEO block molecular weights, M_{PEO} , ranging from 16 to 98 kg/mol. The low-frequency storage modulus (G') at 90 °C increases with increasing M_{PEO} from about 4×10^5 to 5×10^7 Pa. Surprisingly, the conductivity of the SEO/salt mixtures with the molar ratio of Li to ethylene oxide moieties of 0.02 σ , also increases with increasing M_{PEO} , from 6.2×10^{-5} to 3.6×10^{-4} S/cm at 90 °C. We compare σ with the conductivity of pure PEO/salt mixtures, σ_{PEO} , and find that $\sigma/[\phi\sigma_{\text{PEO}}]$ of our highest molecular weight sample is close to 0.67, the theoretical upper limit for transport through randomly oriented lamellar grains.

Introduction

Polymer membranes with high ionic conductivity are important for applications such as solid-state batteries and fuel cells.¹ The performance of these materials depends not only on their electrical properties but also on other properties such as shear modulus, permeability, etc. The mechanical properties of polymer electrolytes, for example, are particularly important in secondary solid-state lithium batteries. Repeated cycling of these systems leads to dendrite formation, reducing battery life and compromising safety.¹ Recent theoretical work indicates that dendrite growth can be stopped if the shear modulus of current polymer electrolytes can be increased by 3 orders of magnitude without a significant decrease in ionic conductivity.^{2–4} Several studies have shown that cation transport is intimately coupled to segmental motion of the polymer chains.^{5,6} High ionic conductivity is obtained in soft polymers such as rubbery poly(ethylene oxide) (PEO) where rapid segmental motion needed for ion transport results in a decrease in the rigidity of the polymer.⁷ There is, thus, a clear need to develop methodologies for decoupling the electrical and mechanical properties of polymer electrolytes.

Several workers have studied the possibility of using PEO-containing block copolymers as electrolytes.^{8–28} In these systems, the conducting pathways are provided by an EO

containing block while a nonconducting block imparts the desired mechanical properties. One example of such a composite electrolyte is shown schematically in Figure 1a, where all of the conducting lamellae are oriented perfectly in the direction of ion transport. The electrical conductivity of this electrolyte is given by

$$\sigma_{\text{max}} = \phi\sigma_{\text{PEO}} \quad (1)$$

where ϕ is the volume fraction of the conducting phase and σ_{PEO} is the conductivity of pure PEO. We call the conductivity of the electrolyte in Figure 1a σ_{max} because any other orientation of the conducting pathways would lead to a lower conductivity. For example, for the orientation shown in Figure 1b, where the conducting channels are orthogonal to the direction of ion transport, the conductivity of the block copolymer would be zero. Equation 1 is based on the assumptions that the conductivity of a PEO nanostructure is identical to that of bulk PEO, and the nanostructures are perfectly aligned relative to the electrodes. In practical applications, which require 25–100 μm thick polymer films, one expects to obtain randomly oriented lamellae. For such cases, it has been argued that $\sigma = (2/3)\sigma_{\text{max}}$.²⁸ We thus anticipate that the improved mechanical properties of block copolymer electrolytes are obtained with a concomitant loss in electrical conductivity.

Many groups have studied copolymers where a nonconducting block is dispersed in a continuous PEO matrix.^{19–23} These composite systems are not of direct interest to this study because their mechanical properties are dominated by the mechanical properties of PEO. On the other hand, if PEO is the minor component, then the mechanical properties of the composite are controlled by the block that forms the major component.

* Corresponding author.

[†] Environmental Energy Technologies Division, Lawrence Berkeley National Laboratory, UC Berkeley.

[‡] Department of Chemical Engineering, UC Berkeley.

[§] Materials Sciences Division, Lawrence Berkeley National Laboratory, UC Berkeley.

[‡] University of Athens.

[#] Argonne National Laboratory.

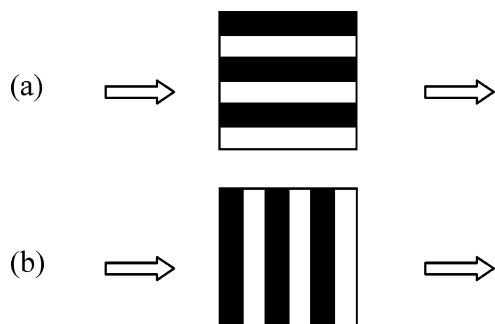


Figure 1. Schematic of a lamellar phase in two different orientations relative to the direction of transport, indicated by the arrows: (a) parallel orientation, (b) orthogonal orientation.

This enables decoupling of mechanical and electrical properties of polymer electrolytes. We thus focus on results obtained in systems where the nonconducting phase is continuous.

Out of the 20 papers that we found on the subject of ion conduction in block copolymers,^{8–27} 13 have either comb graft copolymers with oligomeric PEO chains grafted on one of the blocks^{10,12–15,19–22,24} or low molecular weight PEO-containing macromolecules.^{25–27} The design of these materials is driven by conventional wisdom that the conductivity of PEO homopolymers decreases with increasing molecular weight.²⁹ Attaching several oligomeric PEO chains to one block leads to independent control over the volume fraction of the conducting phase and the molecular weight of the chains within that phase. We refer to these kinds of copolymers as graft–block copolymers (the grafts are invariably oligomeric PEO). In an important systematic study of a variety of graft–block copolymers, Mayes and co-workers^{15–17} report that block copolymers with enhanced conductivity are obtained when the conducting block is attached to a soft rubbery block rather than a hard glassy block. If this is generally true, then the increase in modulus attainable in ionically conducting block copolymers would be extremely limited. The existing literature on polymer electrolytes leads to the following conclusions: (1) The conductivity of composite polymer electrolytes decreases with increasing modulus of the nonconducting block. (2) Ionic conductivity decreases with increasing molecular weight of the polymer electrolyte and levels off in the high molecular weight limit.²⁹

In this work, we report on the electrical and mechanical properties of a series of polystyrene–poly(ethylene oxide) (SEO) block copolymers. Our data enable a critical evaluation of the validity of the conclusions listed above. In particular, we show that the conclusions listed above are not generally valid. The outcome of our work is a strategy for designing block copolymer electrolytes with high modulus and high conductivity that is considerably simpler than the strategies reported in the literature.

Experimental Section

Electrolyte Preparation. The polystyrene–block–poly(ethylene oxide), SEO, diblock copolymers were synthesized via sequential high-vacuum anionic polymerization, using *sec*-butyllithium as the initiator and P4 *tert*-butylphosphazene base as the promoter for the polymerization of ethylene oxide. The synthetic procedure used in this study is described in refs 30 and 31. The number-averaged

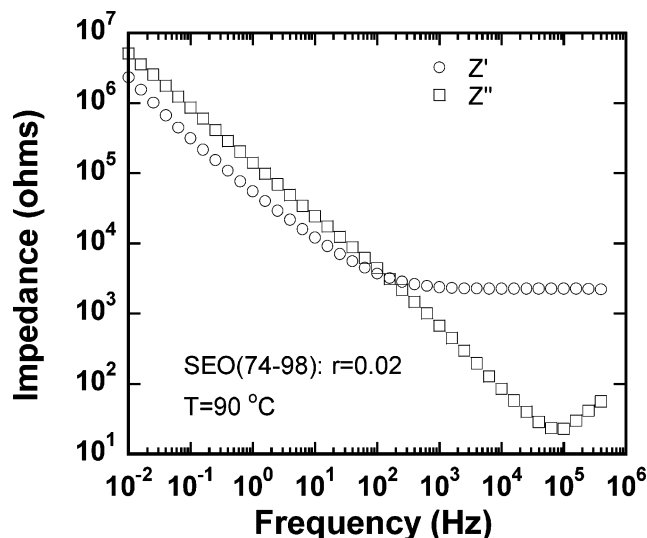


Figure 2. Typical data showing real and imaginary impedance, Z' and Z'' , respectively, as a function of the ac frequency.

molecular weight and the polydispersity index (PDI) of the PS block were obtained using gel permeation chromatography measurements using a Waters 2690 separations module and a Viscotek triple detector system calibrated with polystyrene standards. The PDI of the PS block and the SEO copolymer were found to be less than or equal to 1.10 and 1.20, respectively, for the copolymers studied. The volume fraction of each block was determined using ¹H nuclear magnetic resonance (NMR) spectroscopy. We use SEO(*xx*–*yy*) to denote each diblock copolymer where *xx* and *yy* are the molecular weights of the PS and PEO blocks, respectively, in kg/mol. The PEO homopolymer used in this study (with a number-averaged molecular weight of 20 kg/mol) was purchased from Fluka.

Polymer electrolytes were prepared by blending a SEO/benzene solution with the necessary amount of a 10 wt % solution of Li[N(SO₂CF₃)₂] in THF in an argon glovebox. The solution was freeze-dried in a glovebox-compatible desiccator for 1 week to remove all the solvent. The ratio of Li ions to ethylene oxide moieties, *r*, in our electrolytes was varied from 0.02 to 0.10. The dried SEO/Li[N(SO₂CF₃)₂] mixture was pressed into 1 mm thick disks using a mechanical press with pressures of up to 3000 psi at room temperature. Glovebox integrity was maintained during all of the processing steps. NMR was used to check that the samples were completely dry after completion of the measurements.

Electrolyte Characterization. The ac impedance spectroscopy measurements were made using a homemade test cell on thermostated pressed samples in the glovebox, using a Solartron 1260 frequency response analyzer connected to a Solartron 1296 dielectric interface and blocking stainless steel electrodes. We calculate ionic conductivity from the complex impedance data ($Z^* = Z' - iZ''$) collected at temperatures between 90 and 120 °C where the PEO domains are above their crystalline melting points. All of the samples were annealed at 120 °C for 2 h and cooled to room temperature prior to commencement of the conductivity measurements. The frequency (ω) of the ac voltage was varied from 10^{–2} to 10⁶ Hz. Figure 2 shows a typical plot of real and imaginary impedance, Z' and Z'' , respectively, for SEO(74–98) with *r* = 0.02. At low frequencies, polarization effects result in frequency-dependent impedance data ($Z', Z'' \propto \omega^{-a}$, 0 < *a* < 2).³² At high frequencies the impedance spectra are dominated by ionic mobility,

Table 1. Characteristics of Copolymers Used in This Study

| copolymer | $M_n(\text{PS})$ (g/mol) | $M_n(\text{PEO})$ (g/mol) | ϕ | morphology | <i>d</i> spacing (nm) |
|------------|--------------------------|---------------------------|--------|---------------------------------|-----------------------|
| SEO(36–25) | 36 400 | 24 800 | 0.38 | hexagonally perforated lamellar | 45.2 ± 0.8 |
| SEO(74–98) | 74 000 | 98 100 | 0.55 | lamellar | 98.9 ± 3.4 |
| SEO(40–54) | 39 700 | 53 700 | 0.55 | lamellar | 66.4 ± 1.4 |
| SEO(40–31) | 39 700 | 31 300 | 0.42 | hexagonally perforated lamellar | 39.9 ± 0.6 |
| SEO(16–16) | 16 200 | 16 300 | 0.48 | lamellar | 30.4 ± 0.3 |

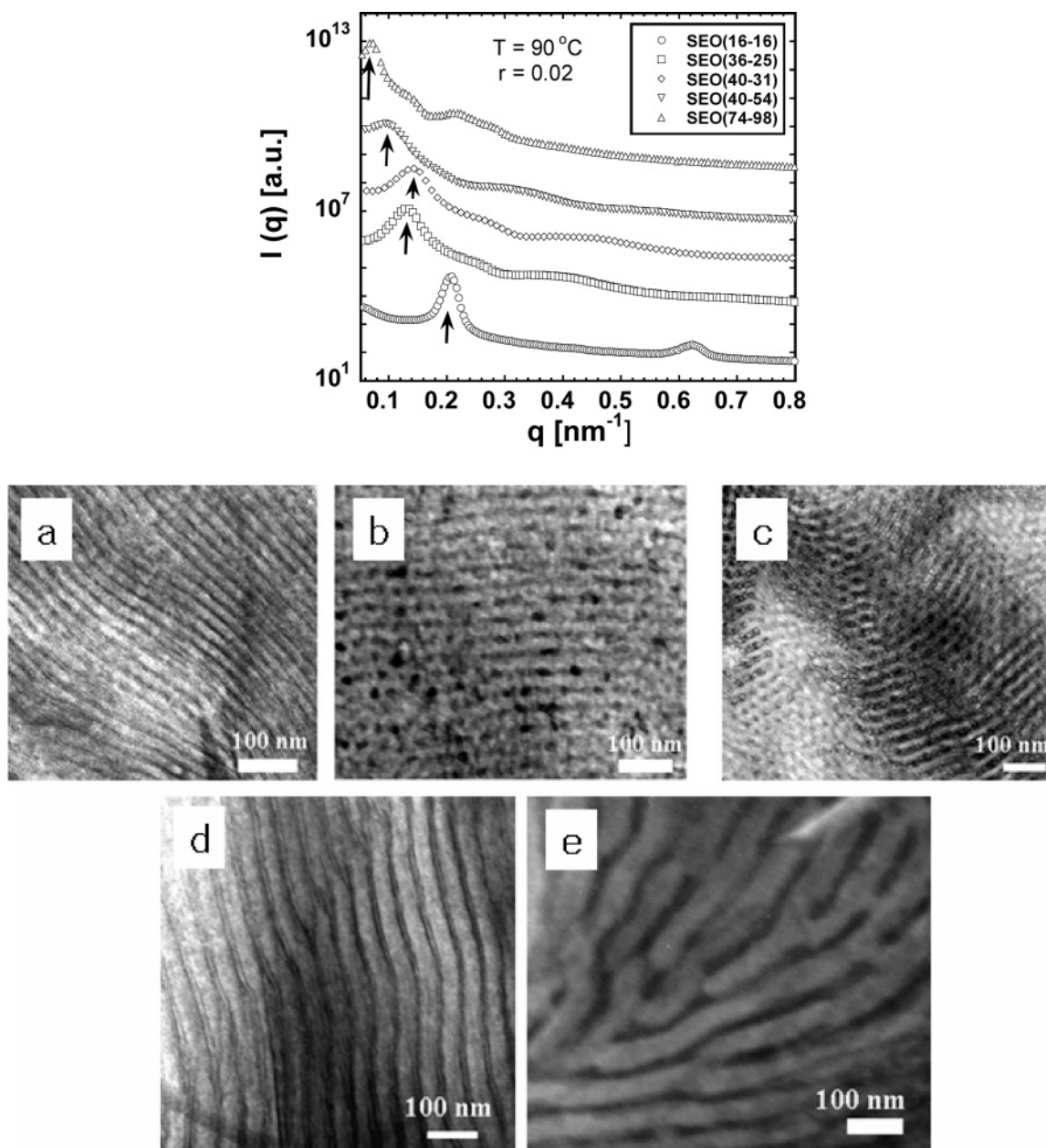


Figure 3. (a, upper) SAXS profiles at 90°C obtained from SEO/salt mixtures with $r = 0.02$. The SAXS data are displaced vertically for clarity. The primary scattering peak for each sample is identified by an arrow. (b, lower) Transmission electron micrographs of the pure SEO copolymers: (a) SEO(16–16), (b) SEO(36–25), (c) SEO(40–31), (d) SEO(40–54), (e) SEO(74–98). The PEO phase is darkened by RuO_4 staining.

resulting in a Z' plateau. The bulk resistance of the electrolyte, R , is read as the high-frequency plateau in the real impedance data,³² and the ionic conductivity is given by

$$\sigma = \frac{L}{RA} \quad (2)$$

where L is the electrolyte thickness and A is the area in contact with the current collectors. The reported results are indistinguishable from those based on the diameters of Z' vs Z'' Nyquist plot semicircles to determine R . The ac voltage amplitude was varied from 10 to 200 mV for each sample to ensure that the impedance measurements were made in the linear regime.

Rheological measurements were performed using an ARES rheometer from Rheometric Scientific Inc. with parallel plate geometry. The annealing history for the rheological and conductivity measurements was identical. Approximately 1 mm thick samples were placed between 8 mm diameter plates for SEO, and 50 mm diameter plates for PEO, in a closed oven with an N_2 atmosphere. The salt-containing SEO samples were exposed to the atmosphere

for about 2 min when they were transferred from the glovebox to the rheometer. All other experiments on SEO/salt mixtures were conducted without loss of glovebox integrity.

The morphological characterization of the samples is based on transmission electron microscopy (TEM) and small-angle X-ray scattering (SAXS). Slightly different annealing protocols were used in these experiments to obtain well-ordered samples to facilitate determination of the morphology. For TEM experiments, the polymer samples were subjected to a pressure of ~ 3000 psi at 120°C for 3 min in a hydraulic press. Thin sections (ca. 50 nm) were prepared using an RMC Boeckeler PT XL cryo-ultramicrotome operating at -100°C . The contrast between the PEO and PS domains was enhanced by RuO_4 staining. Imaging was done using a JEOL 200CX microscope operating at 100 kV. SAXS data were obtained at the 15-ID-D beamline at the Advanced Photon Source (APS) at Argonne National Laboratory, Argonne, IL, using hermetically sealed samples. The samples were annealed in an oven at 145°C for 4 h, cooled to room temperature, and transferred to the beamline. The data were obtained as a function of decreasing temperature, starting at 140°C .

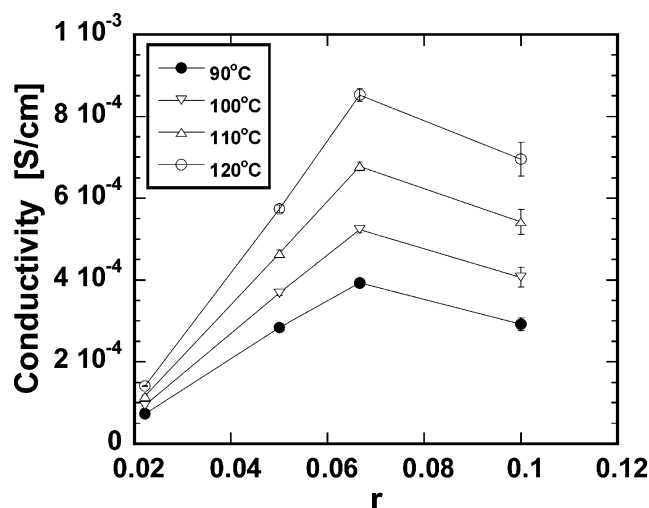


Figure 4. Ionic conductivity vs salt content ranging from $r = 0.02$ to $r = 0.10$ of SEO(36–25) at selected temperatures.

Results and Discussion

Table 1 lists the characteristics of the different SEO copolymers used in this study. We present experimental results obtained by TEM, SAXS, ac impedance spectroscopy, and rheology. Because of the lack of qualitative changes in properties with salt concentration, we focus on data obtained at $r = 0.02$. The ac impedance data obtained from mixtures of a 20 kg/mol PEO homopolymer and $\text{Li}[\text{N}(\text{SO}_2\text{CF}_3)_2]$, and rheological data obtained from pure PEO, serve as the baseline for evaluating the properties of our composite electrolyte. Because of the hygroscopic nature of the salt, extreme precautions were taken to avoid moisture contamination in our samples (see Experimental Section).

In Figure 3a we show SAXS data obtained from SEO/salt mixtures with $r = 0.02$. SAXS data obtained from pure SEO samples were indistinguishable from the data shown in Figure 3a. In each case, we observe a primary scattering peak at $q = q_m$, indicated by arrows in Figure 3a. The SAXS profile of SEO(16–16) with a higher order scattering peak at $3q_m$ indicates the presence of a symmetric lamellar phase ($2q_m$ peak is absent due to a minimum in the form factor of the lamellae). However, long-range order as gauged by the presence of sharp primary and higher order peaks is lacking in all of the other samples. We attribute this to slow diffusion in strongly segregated block copolymers and the complexity of morphologies found in the vicinity of $\phi = 0.40$.^{33–35} The morphology of our samples was thus further clarified by TEM. Typical micrographs obtained from the SEO copolymers, shown in Figure 3b, indicate that SEO(36–25) and SEO(40–31) have a hexagonally perforated lamellar morphology while the other samples have a simple lamellar morphology. There is good agreement between the length scale of the periodic structures, d , determined by SAXS ($d = 2\pi/q_m$) and TEM. On the basis of the similarity in the SAXS profiles obtained with and without salt, we conclude that the addition of salt at low concentrations does not affect the morphology of the SEO copolymers. (We were unable to study the morphology of SEO/salt mixtures by TEM due to lack of access to a moisture-free microtoming facility. Attempts to address this limitation are currently underway.) The TEM and SAXS data rule out the presence of an interpenetrating network phase in our electrolytes.

In Figure 4 we show the dependence of ionic conductivity on r in SEO(36–25). The conductivity has a maximum at $r \approx 0.067$, regardless of the temperature. At low salt concentrations,

ionic conductivity increases with salt concentration due to the increase in the number of charge carriers. At high salt concentrations, transient cross-linking of the polymer chains and neutral ion pairs result in reduced conductivity.⁶ This trend is qualitatively similar to that observed in PEO homopolymer/salt systems.^{36,37}

In Figure 5a we plot the conductivity of our electrolytes, σ , as a function of M_{PEO} , the average molecular weight of the PEO chains, at a fixed value of $r = 0.02$. We find a systematic increase in conductivity with M_{PEO} in the SEO-based electrolytes with no indication of a plateau in the range of molecular weights studied. The observed trend is opposite to that obtained in PEO homopolymer/salt mixtures, where the conductivity decreases with increasing molecular weight and reaches a plateau for molecular weights above 1 kg/mol.²⁹ Data obtained from the PEO homopolymer/salt mixtures with $r = 0.02$ are shown in Figure 5b. In Figure 5c, we plot $\sigma/\sigma_{\text{max}}$ vs M_{PEO} , where $\sigma_{\text{max}} = \phi\sigma_{\text{PEO}}$ (eq 1). The PEO volume fraction in our SEO electrolytes varies from 0.38 to 0.55. The ratio $\sigma/\sigma_{\text{max}}$ normalizes the measured conductivity for the expected linear increase in σ with increasing ϕ . It is evident from Figure 5c that $\sigma/\sigma_{\text{max}}$ increases with M_{PEO} ; i.e. the ionic conductivity of the SEO electrolytes is mainly affected by M_{PEO} and not by block copolymer composition. It is worth noting that σ is a function of both M_{PEO} and temperature (Figure 5a), while $\sigma/\sigma_{\text{max}}$ is only a function of M_{PEO} (Figure 5c).

In an attempt to explain the reason behind the observed relationship between the molecular weight of the PEO block and ionic conductivity, we examine the factors that govern the ionic conductivity of SEO/salt mixtures. They are (1) degree of dissociation of the $\text{Li}[\text{N}(\text{SO}_2\text{CF}_3)_2]$ salt, (2) diffusion coefficients of the dissociated ions (Li^+ and $[\text{N}(\text{SO}_2\text{CF}_3)_2]^-$) in the nanoscale PEO channels, and (3) accessibility and nature of the diffusive paths used by the ions as they travel through the electrolyte. We do not have any direct measurements of the degree of dissociation of the salt. The dissociation of the salt depends on the local dielectric properties of the medium. The dielectric constant of PEO is higher than that of PS, and we expect the salt to reside exclusively in the PEO domains. It is intuitive to anticipate gradients in the dielectric properties of the PEO domains with a lower dielectric constant near the PS interface when compared to that near the center of PEO lamellae. There are two possible reasons for this. (1) It is easier for dipoles on the PEO chains to reorient when they are far from the interface as PEO chains have limited mobility at the interface. (2) A higher dielectric constant at the center of the PEO lamellae would bring more ion pairs to the center, further increasing the dielectric constant as the ion pairs themselves serve as dipoles. Therefore, the degree of dissociation of $\text{Li}[\text{N}(\text{SO}_2\text{CF}_3)_2]$ would be less in the “interfacial volume” near the junctions of the PS and PEO blocks, compared to the rest of the PEO domains. The PS–PEO interfacial area per unit volume decreases with increasing molecular weight. In addition, the interfaces become more sharply defined with increasing molecular weight due to increased segregation between the blocks. These factors lead to the conclusion that the increase in conductivity with M_{PEO} may be due to the expected increase in the concentration of dissociated ions with increasing M_{PEO} .

An increase in Li^+ diffusion coefficient with increasing molecular weight may also lead to the observed trend in Figure 5. It has been argued that dissociated Li^+ ions are tightly coordinated with the ether linkages in PEO,³⁸ and disruption of this coordination could lead to faster ion transport. This disruption may be due to (1) the presence of polystyrene/poly-

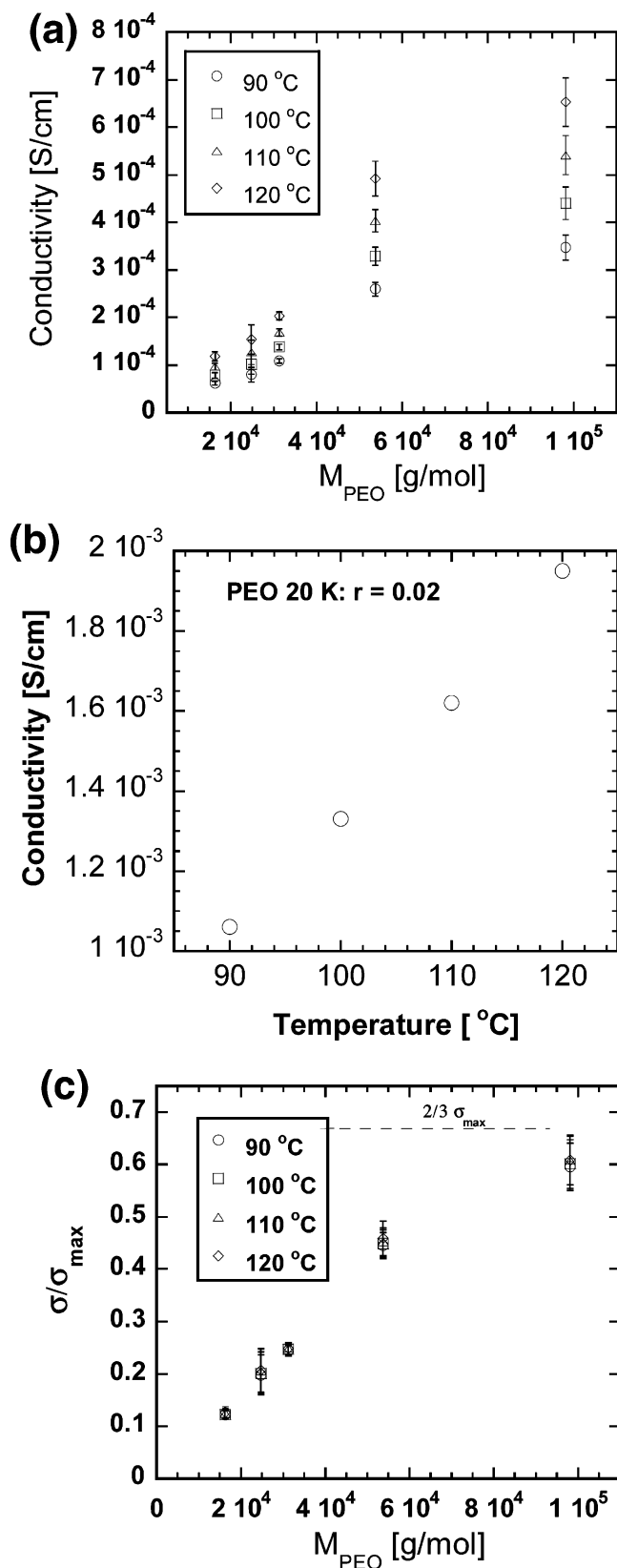


Figure 5. (a) Ionic conductivity of SEO/salt mixtures with $r = 0.02$ vs M_{PEO} at selected temperatures. (b) Ionic conductivity for PEO homopolymer/salt mixtures with $r = 0.02$ at selected temperatures. (c) Normalized ionic conductivity $\sigma/\sigma_{\text{max}}$ vs M_{PEO} where σ_{max} is given by the product $\phi\sigma_{\text{PEO}}$.

(ethylene oxide) interfaces or (2) changes in conformation of the PEO chains due to self-assembly. We know that the interfacial area per unit volume decreases with increasing

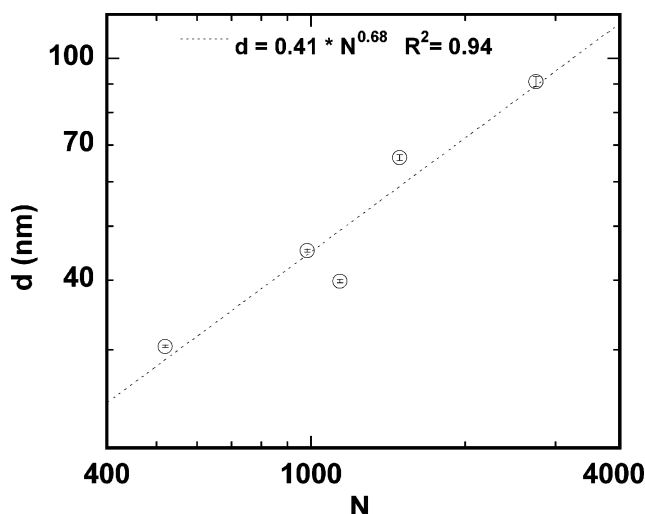


Figure 6. Log-log plot of the domain spacing, d , vs chain length N for the SEO/salt mixtures with $r = 0.02$.

molecular weight. Thus, the changes in Li^+ /PEO coordination in the interfacial region cannot be the reason for the observed increase in ionic conductivity with increasing M_{PEO} . In contrast, it is known that block copolymer chains stretch when they form ordered phases due to the traditional balance of energy and entropy.³⁹ The extent of stretching depends on copolymer chain length, N , and the Flory-Huggins interaction parameter between the blocks, χ . (We use a reference volume of 0.1 nm^3 as the basis for both χ and N .) The product χN in our SEO diblock copolymers ranges from 25 to 130 at 90 °C,^{40,41} indicating that our systems are not in the weak segregation limit. An indication of the stretched nature of our PEO chains is the scaling of the domain spacing, d , with N , the average number of 0.1 nm^3 monomers per chain.⁴² In Figure 6, we plot d vs N . A least-squares power law fit yields $d \text{ (nm)} = 0.41N^{0.68}$ (both the prefactor and exponent were free parameters in the fit), which is the expected result in the strongly segregated limit.³⁹ We propose that the stretched PEO chains in our high molecular weight block copolymers may not be as tightly coordinated with Li^+ ions as PEO chains in the low molecular weight copolymers, which, in turn, leads to enhanced Li^+ diffusion coefficients. Some support for this proposal is contained in computer simulations of charge transport in stretched PEO chains.⁴³

The observed ionic conductivity can be related to the diffusion of ions in the nanostructured domains following the work of Sax and Ottino.²⁸ The materials studied in ref 28 were polycrystalline, composed of randomly oriented lamellar block copolymer grains, and transport occurred exclusively in one of the lamellae. The authors argued that diffusion in these materials would be slower than that in a pure material by a factor of $2/3$, irrespective of the average grain size, because one-third of the random diffusive steps are not effective for transport. On the basis of these arguments, it follows that $\sigma/\sigma_{\text{max}} = 2/3$. It is reasonable to assume that our samples are polycrystalline because we have not taken any steps to align the lamellae. The azimuthally symmetric SAXS patterns and TEM data presented in Figure 3 support our assumption. It is interesting to note that the value of $\sigma/\sigma_{\text{max}}$ of the SEO(74–98)-based electrolyte, our most conductive electrolyte, is close to the theoretical maximum value of 0.67. Since we have not yet characterized the grain structure of our samples, we cannot rule out the possibility that the observed trend in Figure 5 is due to differences in grain structure.

Our experimental results lead to two remarkable conclusions: (1) it is possible to make self-assembled conducting

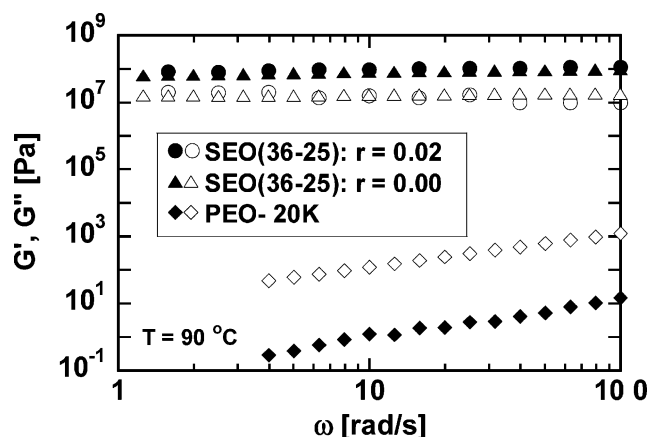


Figure 7. Rheological measurements on SEO(36-25) (triangles), SEO(36-25)/salt with $r = 0.02$ (circles), and PEO (diamonds) samples at 90 °C. Storage modulus $G'(\omega)$ is shown with filled symbols, and the loss modulus $G''(\omega)$ is shown with hollow symbols.

nanostructured electrolytes with continuous high modulus nonconducting phases, and (2) the magnitude of the conductivity of such electrolytes is in the range of the theoretical upper limit that can be expected from such systems. It is important to note that our samples have not been subjected to any special processing steps to ensure that the PEO lamellae are connected or aligned. Connectivity of the PEO phase occurs reproducibly by quiescent annealing at 120 °C. It has been suggested that highly connected network phases are essential for high conductivity.^{9,19,44} We show here that this is not the case.

In Figure 7 we show the frequency (ω) dependence of the storage and loss shear moduli, G' and G'' , respectively, of the pure SEO(36-25), SEO(36-25) with $r = 0.02$, and the pure PEO homopolymer. The data obtained from the pure SEO(36-25) and SEO(36-25) with $r = 0.02$ are indistinguishable. The frequency independence of the moduli and the fact that G' is an order of magnitude larger than G'' indicate that our composite electrolytes are, to a good approximation, elastic solids. The data in Figure 7 confirm that the addition of small amounts of salt has no detrimental effect on the mechanical properties of our material. The value of G' obtained from our SEO(36-25) electrolytes is 100 times larger than the plateau modulus of pure PEO⁴⁵ and 6 orders of magnitude larger than that of the PEO homopolymer used in this study. (The molecular weight of the PEO homopolymer is similar to that of the PEO block in the SEO(36-25) copolymer.) In parts a and b of Figure 8, we show the frequency dependence of G' and G'' , respectively, for the series of SEO copolymers studied here. The higher molecular weight copolymers that exhibit high ionic conductivity yield storage shear moduli on the order of 10^8 Pa. It is evident that the mechanical properties of the electrolytes are governed primarily by the PS phase. By adding the PS block to the PEO chain, we have demonstrated independent control over the mechanical and electrical properties of the electrolyte. In particular, we have shown that the shear modulus of the electrolyte can be increased by several orders of magnitude with relatively little change in ionic conductivity.

Comparison with Literature on Block Copolymer Electrolytes. In order to evaluate the properties of block copolymer electrolytes, it is essential to obtain an accurate measure of the conductivity of pure PEO, σ_{PEO} . Below the crystalline melting temperature of the PEO/salt mixture, one might expect conductivity values that depend on processing history because many aspects of the crystalline phase of polymers such as spherulite size, crystal fraction, long period, etc., are affected by process-

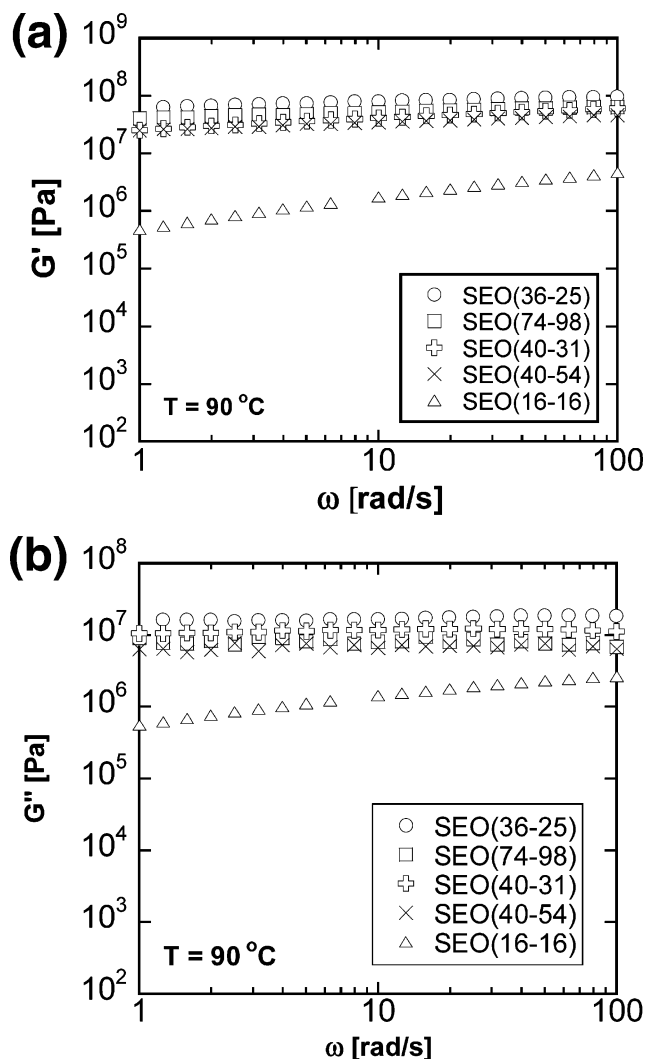


Figure 8. Frequency, ω , dependence of the (a) storage, G' , and (b) loss moduli, G'' , of SEO copolymers.

ing. Volel et al.⁴⁶ have conducted systematic studies of the effect of sample preparation methods on charge transport in amorphous PEO/salt mixtures. They obtained samples by drying the polymer electrolyte from two different solvents—acetonitrile and methyl formate—and obtained different transport properties at temperatures both below and above the melting temperature. This was attributed to different distributions of physical cross-links that arise due to the coordination between Li^+ ions and ethylene oxide moieties on different chains. It is therefore not surprising that literature values of σ_{PEO} of the amorphous state vary by about a factor of 5.^{16,47} These results indicate the importance of quantification of pure PEO/salt mixtures when reporting the conductivity of composite electrolytes.

Given the fact that the motivation for studying block copolymers is to exert independent control over the electrical and mechanical properties of the electrolyte, it is important to measure both properties simultaneously. Because of the complexity of the materials, it is important to obtain conductivity from frequency-dependent ac impedance measurements,³² and modulus using frequency-dependent rheological measurements, rather than values obtained from measurement at an isolated frequency.⁴⁸ In an important publication, Mayes and co-workers evaluated the mechanical and electrical properties of graft-block copolymer electrolytes with poly[oligo(oxyethylene) methacrylate] (POEM) as the conducting block and a soft poly-(laurel methacrylate) nonconducting block.¹⁷ Values of $\sigma/\sigma_{\text{max}}$

as high as 1 ($r = 0.05$) were reported in ref 15 based on frequency-dependent ac impedance. However, the elastic shear modulus (G') of the copolymer reaches a low-frequency plateau of about 10^4 Pa, which is significantly lower than those reported in the present study.

We were not able to find any other study on block copolymer electrolytes where both σ and G' were obtained from frequency-dependent measurements, and the conductivity of the block copolymer was compared with explicit conductivity measurements on the homopolymer. In ref 12, Wang et al. studied the properties of graft-block copolymer electrolytes with poly[oligo(oxyethylene)styrene] (POES) as the conducting block and PS as the nonconducting block. σ/σ_{\max} values of ~ 0.4 ($r = 0.05$) and tensile modulus of 10^8 Pa are reported. Unfortunately, the tensile modulus was not based on frequency-dependent measurements, and thus the true low-frequency modulus of the copolymer may differ substantially from that reported in ref 12. In addition, the volume fraction of the PEO phase, which can readily be estimated from the electron micrograph (Figure 2 of ref 12), is about 0.75, which is significantly different from the 0.60 value reported by the authors. In ref 20, Niitani and co-workers studied the properties of a copolymer with POEM as the conducting phase and PS as the nonconducting phase. They reported a σ value of 3×10^{-5} S/cm ($r = 0.05$) and tensile modulus of 2×10^7 Pa for a copolymer with 55% PEO. The tensile modulus was not based on frequency-dependent measurements, the temperature at which the measurements were made was not specified, and the conductivity of the pure homopolymer was not measured. All other papers on block copolymer electrolytes only report conductivity values. Khan et al.¹⁴ studied a graft-block copolymer with POEM as the conducting phase and PS as the insulating phase and reported $\sigma = 10^{-6}$ S/cm ($r = 0.06$) at 25 °C. Kosonen et al.¹³ studied a graft-block copolymer with poly[oligo(oxyethylene)-4-vinylpyridine] as the conducting phase and PS as the insulating phase and report $\sigma = 10^{-4}$ S/cm ($r = 0.08$) at 80 °C. The main conclusion of ref 13 was that short PEO grafts lead to higher conductivity than long PEO grafts.

It is clear that the dependence of conductivity and modulus on molecular weight of the SEO copolymers reported in the present paper are qualitatively different from previous literature results.

Conclusion

Nanostructured polymer electrolytes with soft conducting channels embedded in a hard electrically insulating matrix are promising candidates for applications that require independent control over mechanical and electrical properties. By showing that network phases are not necessary to obtain ionic conductivity, we have introduced the possibility of using a wide variety of morphologies for designing ionically conducting polymers. No special processing is needed to create percolating conducting pathways in these materials; they are formed entirely by quiescent self-assembly. An important limitation of the present work, and that of all previous work in this field,^{8–27} is that the pathways of ion conduction, i.e., the density of defects, their geometrical characteristics, average grain size, etc., have not yet been determined. Systematic studies of grain structure are restricted to salt-free block copolymers.^{49–51} In future work we will try to quantify the defect structure of salt-containing block copolymers. Despite the limitations, we believe that Li[N(SO₂-CF₃)₂]-doped high molecular weight PS-PEO block copolymers studied here provide an avenue for solving the problem of dendrite growth in Li-polymer batteries.

Acknowledgment. This work was conducted within the Batteries for Advanced Transportation Technologies (BATT) Program, supported by the U.S. Department of Energy Freedom-CAR and Vehicle Technologies Program. TEM was performed at National Center for Electron Microscopy at LBNL. Use of the Advanced Photon Source (APS) was supported by the U.S. Department of Energy, Office of Science, Office of Basic Energy Sciences, under Contract DE-AC02-06CH11357. The SAXS experiments were conducted at the ChemMatCARS Sector 15 of APS which is principally supported by the National Science Foundation/Department of Energy under Grant CHE-0535644. We thank Prof. John Newman, Dr. John Kerr, and Dr. Gao Liu for helpful discussions and the University of California, Berkeley, College of Chemistry machine and electrical shops for their technical assistance.

References and Notes

- (1) Tarascon, J. M.; Armand, M. *Nature (London)* **2001**, *414*, 359–367.
- (2) Monroe, C.; Newman, J. J. *Electrochem. Soc.* **2003**, *150*, A1377–A1384.
- (3) Monroe, C.; Newman, J. J. *Electrochem. Soc.* **2005**, *152*, A396–A404.
- (4) Monroe, C.; Newman, J. J. *Electrochem. Soc.* **2004**, *151*, A880–A886.
- (5) Watanabe, M.; Sanui, K.; Ogata, N.; Kobayashi, T.; Ohtaki, Z. *J. Appl. Phys.* **1985**, *57*, 123–128.
- (6) Kakihana, M.; Schantz, S.; Torell, L. M. *J. Chem. Phys.* **1990**, *92*, 6271–6277.
- (7) Boden, N.; Leng, S. A.; Ward, I. M. *Solid State Ionics* **1991**, *45*, 261–270.
- (8) Epps, T. H.; Bailey, T. S.; Waletzko, R.; Bates, F. S. *Macromolecules* **2003**, *36*, 2873–2881.
- (9) Cho, B. K.; Jain, A.; Gruner, S. M.; Wiesner, U. *Science* **2004**, *305*, 1598–1601.
- (10) Li, J.; Khan, I. M. *Makromol. Chem.* **1991**, *192*, 3043–3050.
- (11) Arbizzani, C.; Mastragostino, M.; Hamaide, T.; Guyot, A. *Electrochim. Acta* **1990**, *35*, 1781–1785.
- (12) Wang, C. X.; Sakai, T.; Watanabe, O.; Hirahara, K.; Nakanishi, T. *J. Electrochem. Soc.* **2003**, *150*, A1166–A1170.
- (13) Kosonen, H.; Valkama, S.; Hartikainen, J.; Eerikainen, H.; Torkkeli, M.; Jokela, K.; Serimaa, R.; Sundholm, F.; ten Brinke, G.; Ikkala, O. *Macromolecules* **2002**, *35*, 10149–10154.
- (14) Khan, I. M.; Fish, D.; Delaviz, Y.; Smid, J. *Makromol. Chem.* **1989**, *190*, 1069–1078.
- (15) Trapa, P. E.; Won, Y. Y.; Mui, S. C.; Olivetti, E. A.; Huang, B. Y.; Sadoway, D. R.; Mayes, A. M.; Dallek, S. J. *Electrochem. Soc.* **2005**, *152*, A1–A5.
- (16) Trapa, P. E.; Huang, B. Y.; Won, Y. Y.; Sadoway, D. R.; Mayes, A. M. *Electrochem. Solid State* **2002**, *5*, A85–A88.
- (17) Soo, P. P.; Huang, B. Y.; Jang, Y. I.; Chiang, Y. M.; Sadoway, D. R.; Mayes, A. M. *J. Electrochem. Soc.* **1999**, *146*, 32–37.
- (18) Ruzette, A. V. G.; Soo, P. P.; Sadoway, D. R.; Mayes, A. M. *J. Electrochem. Soc.* **2001**, *148*, A537–A543.
- (19) Niitani, T.; Shimada, M.; Kawamura, K.; Dokko, K.; Rho, Y. H.; Kanamura, K. *Electrochem. Solid State* **2005**, *8*, A385–A388.
- (20) Niitani, T.; Shimada, M.; Kawamura, K.; Kanamura, K. *J. Power Sources* **2005**, *146*, 386–390.
- (21) Gray, F. M.; MacCallum, J. R.; Vincent, C. A.; Giles, J. R. M. *Macromolecules* **1988**, *21*, 392–397.
- (22) Giles, J. R. M.; Gray, F. M.; MacCallum, J. R.; Vincent, C. A. *Polymer* **1987**, *28*, 1977–1981.
- (23) Jannasch, P. *Chem. Mater.* **2002**, *14*, 2718–2724.
- (24) Hirahara, K.; Takano, A.; Yamamoto, M.; Kazama, T.; Isono, Y.; Fujimoto, T.; Watanabe, O. *React. Funct. Polym.* **1998**, *37*, 169–182.
- (25) Ohtake, T.; Ogasawara, M.; Ito-Akita, K.; Nishina, N.; Ujiie, S.; Ohno, H.; Kato, T. *Chem. Mater.* **2000**, *12*, 782–789.
- (26) Kishimoto, K.; Yoshio, M.; Mukai, T.; Yoshizawa, M.; Ohno, H.; Kato, T. *J. Am. Chem. Soc.* **2003**, *125*, 3196–3197.
- (27) Wright, P. V.; Zheng, Y.; Bhatt, D.; Richardson, T.; Ungar, G. *Polym. Int.* **1998**, *47*, 34–42.
- (28) Sax, J.; Ottino, J. M. *Polym. Eng. Sci.* **1983**, *23*, 165–176.
- (29) Shi, J.; Vincent, C. A. *Solid State Ionics* **1993**, *60*, 11–17.
- (30) Hadjichristidis, N.; Iatrou, H.; Pispas, S.; Pitsikalis, M. *J. Polym. Sci., Polym. Chem.* **2000**, *38*, 3211–3234.
- (31) Quirk, R. P.; Kim, J.; Kausch, C.; Chun, M. S. *Polym. Int.* **1996**, *39*, 3–10.
- (32) MacCallum, J. R.; Vincent, C. A., Eds.; Elsevier Applied Science Publishers Ltd.: New York, 1987; Vol. 1.

- (33) Lodge, T. P.; Blazey, M. A.; Liu, Z.; Hamley, I. W. *Macromol. Chem. Phys.* **1997**, *198*, 983–995.
- (34) Yokoyama, H.; Kramer, E. J. *Macromolecules* **1998**, *31*, 7871–7876.
- (35) Qi, S. Y.; Wang, Z. G. *Macromolecules* **1997**, *30*, 4491–4497.
- (36) Robitaille, C. D.; Fauteux, D. *J. Electrochem. Soc.* **1986**, *133*, 315–325.
- (37) Gorecki, W.; Belorizky, E.; Berthier, C.; Donoso, P.; Armand, M. *Electrochim. Acta* **1992**, *37*, 1685–1687.
- (38) Gray, F. M. *Solid Polymer Electrolytes. Fundamentals and Technological Applications*; VCH: Weinheim, 1991.
- (39) Helfand, E.; Wasserman, Z. R. *Developments in Block Copolymers*; Applied Science: London, 1982.
- (40) Zhu, L.; Cheng, S. Z. D.; Calhoun, B. H.; Ge, Q.; Quirk, R. P.; Thomas, E. L.; Hsiao, B. S.; Yeh, F.; Lotz, B. *Polymer* **2001**, *42*, 5829–5839.
- (41) The expression for χ is taken from ref 40, and we use a reference volume of 0.1 nm³ to compute both χ and N .
- (42) Balsara, N. P. In *Physical Properties of Polymers Handbook*; Mark, J. E., Ed.; AIP Press: New York, 1996; pp 257–268.
- (43) Borodin, O.; Smith, G. D. *Macromolecules* **2006**, *39*, 1620–1629.
- (44) Epps, T. H.; Bailey, T. S.; Pham, H. D.; Bates, F. S. *Chem. Mater.* **2002**, *14*, 1706–1714.
- (45) Fetters, L. J.; Lohse, D. J.; Richter, D.; Witten, T. A.; Zirkel, A. *Macromolecules* **1994**, *27*, 4639–4647.
- (46) Volel, M.; Armand, M.; Gorecki, W. *Macromolecules* **2004**, *37*, 8373–8380.
- (47) Lascaud, S.; Perrier, M.; Vallee, A.; Besner, S.; Prudhomme, J.; Armand, M. *Macromolecules* **1994**, *27*, 7469–7477.
- (48) Ferry, J. D. *Viscoelastic Properties of Polymers*; Wiley: New York, 1980.
- (49) Gido, S. P.; Gunther, J.; Thomas, E. L.; Hoffman, D. *Macromolecules* **1993**, *26*, 4506–4520.
- (50) Gido, S. P.; Thomas, E. L. *Macromolecules* **1994**, *27*, 6137–6144.
- (51) Balsara, N. P.; Garetz, B. A.; Dai, H. J. *Macromolecules* **1992**, *25*, 6072–6074.

MA0629541